Critical Behavior and Fractality in Shallow One-Dimensional Quasiperiodic Potentials

Hepeng Yao, Alice Khoudli, Léa Bresque, and Laurent Sanchez-Palencia
CPHT, CNRS, Ecole Polytechnique, Institut Polytechnique de Paris, Route de Saclay, F-91128 Palaiseau, France

(Received 2 April 2019; published 16 August 2019)

Quasiperiodic systems offer an appealing intermediate between long-range ordered and genuine disordered systems, with unusual critical properties. One-dimensional models that break the so-called self-dual symmetry usually display a mobility edge, similarly as truly disordered systems in a dimension strictly higher than two. Here, we determine the critical localization properties of single particles in shallow, one-dimensional, quasiperiodic models and relate them to the fractal character of the energy spectrum. On the one hand, we determine the mobility edge and show that it separates the localized and extended phases, with no intermediate phase. On the other hand, we determine the critical potential amplitude and find the universal critical exponent $\nu \simeq 1/3$. We also study the spectral Hausdorff dimension and show that it is nonuniversal but always smaller than unity, hence showing that the spectrum is nowhere dense. Finally, applications to ongoing studies of Anderson localization, Bose-glass physics, and many-body localization in ultracold atoms are discussed.

DOI: 10.1103/PhysRevLett.123.070405

In a homogeneous system, all the single-particle wave functions are extended. In contrast, they may be exponentially localized in the presence of disorder owing to the breaking of translational invariance [1]. This effect, known as Anderson localization, is a fundamental, ubiquitous phenomenon at the origin of metal-insulator transitions in many systems [2]. Quasiperiodic models hold a special place, for they are at the interface of long-range ordered and fully disordered systems. They describe a variety of systems, including quasicrystals [3], electronic materials in orthogonal magnetic fields [4–6] or with incommensurate charge-density waves [7], Fibonacci heterostructures [8], photonic crystals [9], and cavity polaritons [10]. They also proved pivotal in quantum gases [11–13] to investigate Anderson localization of matter waves [14–16] and interacting Bose gases [17], the emergence of long-range quasiperiodic order [18–20], Bose-glass physics [14,15,21–24], and many-body localization [25–28].

Anderson localization in quasiperiodic systems, however, significantly differs from its counterpart in truly disordered systems. While in a disordered system a phase transition between the Anderson-localized and extended phases occurs only in a dimension strictly higher than 2 [29], it may occur in one-dimensional (1D) quasiperiodic systems. The most celebrated example is the Aubry-André (AA) Hamiltonian, obtained from the tight-binding model generated by a strong lattice, by adding a second, weak, incommensurate lattice. In the AA model, the localization transition occurs at a critical value of the quasiperiodic potential, irrespective of the particle energy [30]. This behavior results from a special symmetry, known as self-duality. When the latter is broken, an energy mobility edge (ME), i.e., a critical energy separating localized and extended states, generally appears, as demonstrated in a variety of models [31–38]. One of the simplest examples is obtained by using two incommensurate lattices of comparable amplitudes. This model attracts significant attention in ultracold-atom systems [39,40]. They have been used to study many-body localization in a 1D system exhibiting a single-particle ME [28] and may serve to overcome finite-temperature issues in the observation of the still elusive Bose-glass phase [24,41] (see below). Recently, the localization properties and the ME of the single-particle problem have been studied both theoretically [40] and experimentally [42]. However, important critical properties of this model are still unknown. For instance, whether an intermediate phase appears in between the localized and extended phases remains unclear.

In this work, we study the critical properties and the fractality of noninteracting particles in shallow quasiperiodic potentials. We consider various models, including bichromatic and trichromatic lattices with balanced or imbalanced amplitudes. In all cases, above a certain critical amplitude of the quasiperiodic potential V_c, we find a finite energy ME. It marks a sharp transition between the localized and extended phases with no intermediate phase. The ME is always found in one of the energy gaps, which are dense. We show that this is a direct consequence of the fractal character of the energy spectrum, which is nowhere dense. We compute the critical Hausdorff dimension and find values significantly different from that found for the AA model, showing that it is a nonuniversal quantity. Moreover, we determine accurate values of the critical quasiperiodic amplitude V_c from the scaling of the inverse participation ratio. While V_c depends on the model, we find the universal critical exponent $\nu \simeq 1/3$.

Model and approach.—The single-particle wave functions $\psi(x)$ are found by solving numerically the continuous-space, 1D Schrödinger equation:

$$E\psi(x) = -\frac{\hbar^2}{2m}\frac{d^2\psi}{dx^2} + V(x)\psi(x), \tag{1}$$

using exact diagonalization for Dirichlet absorbing boundary conditions: $\psi_n(0) = \psi_n(L) = 0$. Here, E and m are the particle energy and mass, respectively, L is the system size, and $\hbar$ is the reduced Planck constant. In the first part of this work, we consider the bichromatic lattice potential

$$V(x) = \frac{V_1}{2}\cos(2k_1 x) + \frac{V_2}{2}\cos(2k_2 x + \varphi), \tag{2}$$

where the quantities V_j $(j = 1, 2)$ are the amplitudes of two periodic potentials of incommensurate spatial periods π/k_j with $k_2/k_1 = r$, an irrational number. The relative phase shift φ is essentially irrelevant, except for some values which induce special symmetries. In the following, we use $r = (\sqrt{5}-1)/2$ and $\varphi = 4$, which avoids such cases. We then characterize the localization of an eigenstate ψ using the second-order inverse participation ratio (IPR) [43]:

$$\mathrm{IPR} = \frac{\int dx|\psi_n(x)|^4}{[\int dx|\psi_n(x)|^2]^2}. \tag{3}$$

It generally scales as $\mathrm{IPR} \sim 1/L^\tau$, with $\tau = 1$ for an extended state and $\tau = 0$ for a localized state.

Mobility edge.—We first focus on the balanced bichromatic lattice, Eq. (2) with $V_1 = V_2 \equiv V$. Note that this model cannot be mapped onto the AA model, even for $V \gg E_r$, where $E_r = \hbar^2 k_1^2/2m$ is the recoil energy, since none of the periodic components of $V(x)$ dominates the other. Figure 1(a) shows the IPR versus the particle energy E and the potential amplitude V for a large system, $L = 100a$ with $a = \pi/k_1$ the spatial period of the first periodic potential. The results indicate the onset of localization (corresponding to large values of the IPR) at a low particle energy and high potential amplitude, consistently with the existence of a V-dependent energy ME E_c. This is confirmed by the behaviour of the wave functions, which turn from exponentially localized at low energy [Fig. 1(b)] to extended at high energy [Fig. 1(c)]. These results are characteristic of 1D quasiperiodic models that break the AA self-duality condition [34,39,40]. The IPR, however, varies smoothly with the particle energy and is not sufficient to distinguish extended states from states localized on a large scale.

To determine the ME precisely, we perform a systematic finite-size scaling analysis of the IPR and compute the quantity

$$\tau(L) \equiv -d\log \mathrm{IPR}/d\log L. \tag{4}$$

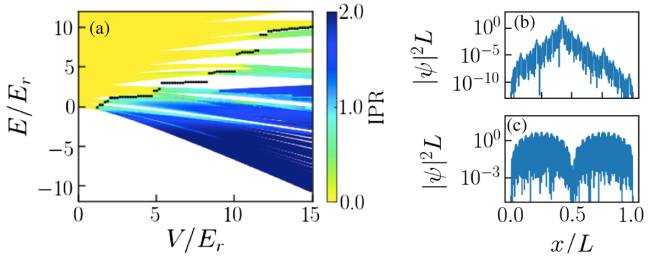

FIG. 1. Localization transition for the balanced bichromatic potential, Eq. (2) with $V_1 = V_2 \equiv V$. (a) IPR versus the particle energy E and the lattice amplitude V for the system size $L = 100a$. Localized states correspond to large values of the IPR (blue) and extended to vanishingly small values (yellow). The ME, found from a finite-L scaling analysis of the IPR, is shown as black points. (b),(c) Density profiles of two eigenstates in the localized and extended regimes, respectively. Here, the two states correspond to energies right below and right above the ME at $V = 2E_r$.

For all values of V and E, and for large enough system lengths, we find either $\tau = 0 \pm 0.2$ or $\tau = 1 \pm 0.2$ [44]. It shows the existence of a sharp localization transition (ME) between localized states ($\tau \simeq 0$) at a low energy and extended states ($\tau \simeq 1$) at a high energy. No intermediate behavior is found in the thermodynamic limit. The ME E_c is then accurately determined as the energy of the transition point between the two values.

The results are plotted in Fig. 1(a) (black dots). In all cases, we find that the ME is in an energy gap. While it is clearly seen for some potential amplitudes (e.g., for $5.2 \lesssim V/E_r \lesssim 8.5$), it is more elusive for some other values (e.g., for $V/E_r \gtrsim 8.5$); see Fig. 1(a). In the latter case, however, it can be seen by enlarging the figure [44]. More fundamentally, it is a direct consequence of the fractal behavior of the energy spectrum, as we discuss now.

Fractality of the energy spectrum.—To characterize the energy spectrum, we first compute the integrated density of states (IDOS) per unit lattice spacing $n_\epsilon(E)$, i.e., the number of eigenstates in the energy range $[E - \epsilon/2, E + \epsilon/2]$, divided by L/a. Figures 2(a) and 2(b) show the quantity $n_\epsilon(E)/\epsilon$ in the vicinity of the ME for two values of the quasiperiodic amplitude V and several energy resolutions ϵ [45]. For any value of ϵ, the IDOS displays energy bands separated by gaps. However, when the resolution ϵ decreases (corresponding to increasingly dark lines on the plots), new gaps appear inside the bands, while the existing gaps are stable. It signals that the spectrum is nowhere dense while the gaps are dense in the thermodynamic limit. In particular, the density of states $\lim_{\epsilon\to 0_+} n_\epsilon(E)/\epsilon$ is singular. Moreover, the ME is always found in a gap for a sufficiently resolved spectrum; see Figs. 2(a) and 2(b). Note that this is not a finite-size effect: For all the results shown here, we have used large enough systems so that each ϵ-resolved band contains at least 10–15 states. In addition, we have checked that the IDOS is stable against further

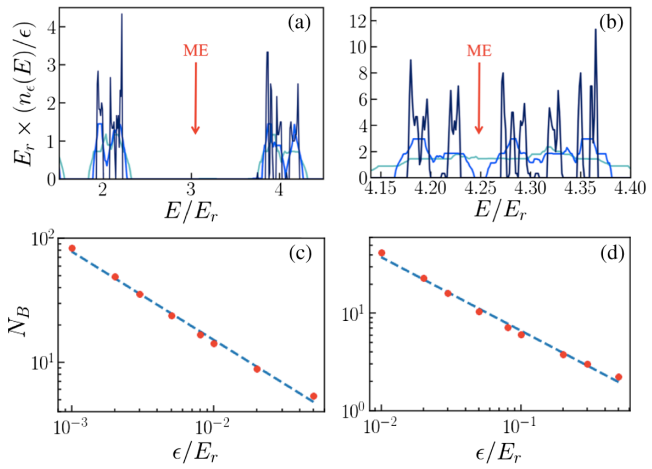

FIG. 2. Fractal behavior of the energy spectrum. (a) shows $n_\epsilon(E)/\epsilon$ in the vicinity of the ME at $V = 6.0E_r$ for $L = 600a$ and $\epsilon/E_r = 0.1$ (light blue), 0.05 (blue), and 0.01 (dark blue). (b) shows the same quantity for the ME at $V = 8.5E_r$ for $L = 1000a$ and $\epsilon/Er = 0.1$ (light blue), 0.03 (blue), and 0.003 (dark blue). (c) and (d) show the energy-box counting number N_B versus ϵ for the parameters of (a) and (b), respectively. The linear slopes in the log-log scale are consistent with a fractal behavior [Eq. (6)] with $D_H = 0.72 \pm 0.03$ and $D_H = 0.76 \pm 0.03$, respectively.

increasing the system's length [44]. The opening of an infinite series of minigaps is characteristic of a fractal behavior.

So far, the fractal character of the energy spectrum of 1D incommensurate systems has been studied for discrete models, such as the Fibonacci chain and the AA model [6,10,46–49]. It was shown that in these cases the spectrum is homeomorphic to a Cantor set. To study fractality in our continuous model, we use a direct box-counting analysis [50,51]: We introduce the *energy-box counting number*:

$$N_B(\epsilon) = \lim_{q\to 0_+} \int_{E_1}^{E_2} \frac{dE}{\epsilon} [n_\epsilon(E)]^q, \tag{5}$$

for some energy range $[E_1, E_2]$. In the limit $q \to 0_+$, the quantity $[n_\epsilon(E)]^q$ approaches 1 if $n_\epsilon(E) \neq 0$ and 0 if $n_\epsilon(E) = 0$. Therefore, the quantity $\lim_{q\to 0_+}[n_\epsilon(E)]^q$ contributes 1 in the boxes of width ϵ containing at least one state and vanishes in the empty boxes. The sum of these contributions, $N_B(\epsilon)$, counts the minimal number of ϵ-wide boxes necessary to cover all the states within the energy range $[E_1, E_2]$. The scaling of $N_B(\epsilon)$ versus the energy resolution ϵ,

$$N_B(\epsilon) \sim \epsilon^{-D_H}, \tag{6}$$

defines the Hausdorff dimension D_H of the energy spectrum. In all considered cases, we found a scaling consistent with Eq. (6) with $0 < D_H < 1$. This is characteristic of a nontrivial fractal behavior [52]. For instance, Figs. 2(c) and 2(d) show N_B versus ϵ in the vicinity of the MEs at $V = 6E_r$ and $V = 8.5E_r$ for the energy ranges corresponding to Figs. 2(a) and 2(b), respectively. We find a linear scaling in the log-log scale, consistent with Eq. (6) and the Hausdorff dimensions $D_H = 0.72 \pm 0.03$ and $D_H = 0.76 \pm 0.03$, respectively. Both values are significantly smaller than the geometrical dimension $d = 1$. Therefore, the Lebesgue measure of the energy support vanishes, and the spectrum is nowhere dense in the thermodynamic limit.

Note that the Hausdorff dimension found above significantly differs from that found in previous work at the critical point of the AA model, $D_H \simeq 0.5$ [47,48]. We conclude that the spectral Hausdorff dimension is a nonuniversal quantity. This is confirmed by further calculations we performed. For instance, in the AA limit of our continuous model, $V_1 \gg V_2, E_r$, we recover $D_H = 0.507 \pm 0.005$ at the critical point. Conversely, we found $D_H = 0.605 \pm 0.014$ at the critical point of the balanced lattice (see below).

Criticality.—We now turn to the critical localization behavior. As shown in Fig. 1(a), a finite ME appears only for a potential amplitude V larger than some critical value V_c; see also Ref. [34]. In Fig. 3(a), we plot the IPR of the ground state (IPR_0) versus V. The transition from the extended phase (vanishingly small IPR) to the localized phase (finite IPR) gets sharper when the system size increases and becomes critical in the thermodynamic limit (see darker solid blue lines in the main figure and the inset). Since the IPR scales as $\mathrm{IPR}_0 \sim 1/L$ in the extended phase and as $\mathrm{IPR}_0 \sim 1$ in the localized phase, the critical amplitude can be found with a high precision as the fixed point of $\mathrm{IPR}_0 \times \sqrt{La}$ when increasing the system size L. It yields [44]

$$V_c/E_r \simeq 1.112 \pm 0.002. \tag{7}$$

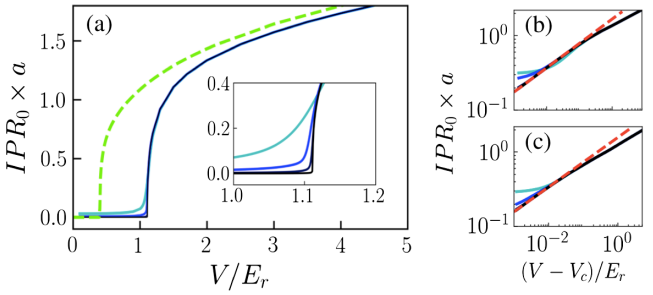

FIG. 3. Critical localization behavior. (a) Ground-state IPR versus the quasiperiodic amplitude for the balanced bichromatic lattice (solid lines). Inset: Magnification in the vicinity of the critical point at V_c. Darker lines correspond to increasing system sizes $L/a = 50$ (light blue), 200 (blue), 1000 (dark blue), and 10000 (black). The dashed green line corresponds to the trichromatic lattice for $L/a = 10000$. (b), (c) Ground-state IPR versus $V - V_c$ in the log-log scale for the bichromatic and trichromatic lattices, respectively.

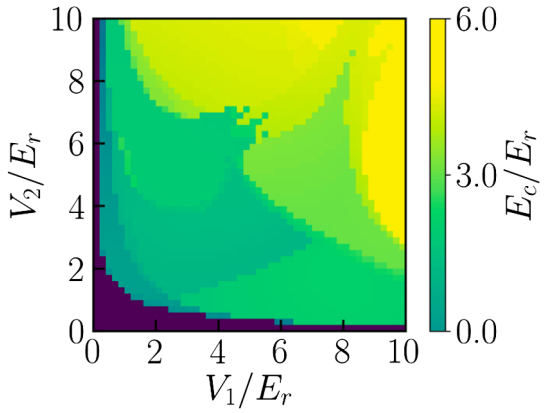

FIG. 4. Mobility edge for the imbalanced bichromatic lattice, Eq. (2) versus the amplitudes V_1 and V_2. The dark region indicates the absence of a mobility edge, and its boundary the localization critical line.

Furthermore, this accurate value of V_c allows us to determine the critical exponent of the transition. Plotting IPR_0 versus $V - V_c$ in the log-log scale, we find a clear linear behavior for sufficiently large systems, consistent with the power-law scaling $\mathrm{IPR}_0 \sim (V - V_c)^\nu$; see Fig. 3(b). Fitting the slope, we find the critical exponent $\nu \simeq 0.327 \pm 0.007$. Note that for $V \gg V_c$, E_r, the behavior of the IPR changes. The ground state is no longer at criticality, and we find the scaling $\mathrm{IPR}_0 \sim V^{\nu'}$ with $\nu' \simeq 0.258 \pm 0.005$. This is consistent with the exponent $1/4$ expected in the tight-binding limit [44].

Other quasiperiodic lattices and universality.—We now extend our results to other quasiperiodic models. We first consider the imbalanced bichromatic lattice, Eq. (2) with $V_1 \neq V_2$. In Fig. 4, we plot the ME versus the quasiperiodic amplitudes V_1 and V_2. The dark region corresponds to cases where the ME is absent. Its boundary yields the critical line in the $V_1 - V_2$ plane. Note that Fig. 4 is not symmetric by exchange of V_1 and V_2 even upon rescaling the energies. This owes to the strong dependence of the model on the incommensurate ratio r. We found that the localization transition is universal, and the critical and fractal properties discussed above for the balanced case apply irrespectively to the relative amplitudes of the two lattices, i.e., also for $V_1 \neq V_2$ [44]. In particular, beyond the critical line, the ME still marks a sharp transition between exponentially localized and extended states, with no intermediate phase. The energy spectrum is fractal, with $D_H < 1$, and thus nowhere dense. Moreover, for any value of V_1 up to values deep in the AA limit ($50E_r$), we always found $\mathrm{IPR}_0 \sim (V_2 - V_{2c})^\nu$ with $\nu \simeq 0.33 \pm 0.02$. The same applies to the discrete AA model [44].

It is worth noting that the behavior of the IPR differs from that of the Lyapunov exponent (inverse localization length). The IPR is dominated by the core of the wave function and characterizes, for instance, the short-range interaction energy of two particles in a localized state [53]. In contrast, the Lyapunov exponent γ characterizes the exponential tails of the wave functions, $\psi(x) \sim \exp(-\gamma|x|)$, and it is insensitive to the core. For nonpurely exponential wave functions, which appear in our model [see, for instance, Fig. 1(b) and Ref. [44]], these two quantities are not proportional. For instance, in the AA model, one has $\gamma \sim \ln(\Delta/2J)$, and, at the critical point $\Delta = 2J$, one finds $\gamma \sim \Delta/2J \sim (V_2 - V_{2c})^\beta$ with the Lyapunov critical exponent $\beta = 1$. This value differs from the IPR critical exponent $\nu \simeq 1/3$ found above.

We also considered the trichromatic lattice

$$V(x) = \frac{V}{2}[\cos(2k_1 x) + \cos(2k_2 x + \varphi) + \cos(2k_3 x + \varphi')], \tag{8}$$

with $k_3/k_2 = k_2/k_1 = r$, so that the three lattice spacings are incommensurate to each other [note that $k_3/k_1 = r^2 = (3 - \sqrt{5})/2$ is an irrational number]. Performing the same analysis as for the other models, we recover the same universal features. In particular, the energy spectrum is fractal and nowhere dense, and the mobility edge is always in a gap. We find a finite critical amplitude V_c and the critical behavior $\mathrm{IPR}_0 \sim (V - V_c)^\nu$ with $\nu \simeq 0.327 \pm 0.007$; see Fig. 3(c). The only significant difference is that the critical point for the trichromatic lattice, $V_c/E_r \simeq 0.400 \pm 0.005$, is smaller than for the bichromatic lattice; see Fig. 3(a). In particular, the standard deviation of the potential, ΔV, is a factor of about 2.27 smaller at the critical point. This is consistent with the intuitive expectation that it should vanish in the disordered case corresponding to an infinite series of cosine components with random phases [54,55].

Conclusion.—In summary, we have studied the critical and fractal behavior for single particles in quasiperiodic potentials. Our results shed light on models that have become pivotal for Anderson [40,42] and many-body [28] localization. We found that the ME is always in a gap and separates localized and extended states, with no intermediate phase. We related this behavior to the fractality of the energy spectrum and found that the Hausdorff dimension is always smaller than unity but nonuniversal. In contrast, we found the critical behavior $\mathrm{IPR}_0 \sim (V - V_c)^\nu$ with the universal exponent $\nu \simeq 1/3$. These predictions may be confirmed in experiments similar to Ref. [42] using energy-resolved state selection [56–58]. In parallel to further theoretical studies, they may help answer questions our results call. For instance, it would be interesting to determine the physical origin of the critical exponent ν and extend our study to higher dimensions. Another important avenue would be to extend it to interacting models in connection to many-body localization.

Our results may also pave the way to the observation of the still elusive Bose-glass phase. So far, ultracold-atom experiments have been performed in the AA limit, the energy scale of which is the tunneling energy J [59]. The

latter is exponentially small in the main lattice amplitude and of the order of the temperature. It suppresses coherence and significantly alters superfluid-insulator transitions [24,41]. In shallow quasiperiodic potentials, the energy scale is, instead, the recoil energy E_r, which is much higher than the temperature. Temperature effects should thus be negligible. For strong interactions, the 1D Bose gas can be mapped onto an ideal Fermi gas, and the Bose-glass transition is directly given by the ME we computed here. It would be interesting to determine how the transition evolves for weak interactions.

We thank David Clément and Thierry Giamarchi for fruitful discussions. This research was supported by the European Commission FET-Proactive QUIC (H2020 Grant No. 641122) and the Paris region DIM-SIRTEQ. This work was performed using HPC resources from GENCI-CINES (Grant No. 2018-A0050510300). We thank the CPHT computer team for valuable support.

[1] P. W. Anderson, Absence of diffusion in certain random lattices, Phys. Rev. **109**, 1492 (1958).
[2] E. Abrahams, *50 Years of Anderson Localization* (World Scientific, Singapore, 2010).
[3] D. Shechtman, I. Blech, D. Gratias, and J. W. Cahn, Metallic Phase with Long-Range Orientational Order and No Translational Symmetry, Phys. Rev. Lett. **53**, 1951 (1984).
[4] R. Peierls, Theory of the diamagnetism of conduction electrons, Z. Phys. **80**, 763 (1933).
[5] P. G. Harper, Single band motion of conduction electrons in a uniform magnetic field, Proc. Phys. Soc. London Sect. A **68**, 874 (1955).
[6] D. R. Hofstadter, Energy levels and wave functions of Bloch electrons in rational and irrational magnetic fields, Phys. Rev. B **14**, 2239 (1976).
[7] J. Wilson, F. Di Salvo, and S. Mahajan, Charge-density waves and superlattices in the metallic layered transition metal dichalcogenides, Adv. Phys. **24**, 117 (1975).
[8] R. Merlin, K. Bajema, R. Clarke, F. Y. Juang, and P. K. Bhattacharya, Quasiperiodic GaAs-AlAs Heterostructures, Phys. Rev. Lett. **55**, 1768 (1985).
[9] Y. Lahini, R. Pugatch, F. Pozzi, M. Sorel, R. Morandotti, N. Davidson, and Y. Silberberg, Observation of a Localization Transition in Quasiperiodic Photonic Lattices, Phys. Rev. Lett. **103**, 013901 (2009).
[10] D. Tanese, E. Gurevich, F. Baboux, T. Jacqmin, A. Lemaitre, E. Galopin, I. Sagnes, A. Amo, J. Bloch, and E. Akkermans, Fractal Energy Spectrum of a Polariton Gas in a Fibonacci Quasiperiodic Potential, Phys. Rev. Lett. **112**, 146404 (2014).
[11] A. Aspect and M. Inguscio, Anderson localization of ultracold atoms, Phys. Today **62**, No. 8, 30 (2009).
[12] G. Modugno, Anderson localization in Bose-Einstein condensates, Rep. Prog. Phys. **73**, 102401 (2010).
[13] L. Sanchez-Palencia and M. Lewenstein, Disordered quantum gases under control, Nat. Phys. **6**, 87 (2010).
[14] B. Damski, J. Zakrzewski, L. Santos, P. Zoller, and M. Lewenstein, Atomic Bose and Anderson Glasses in Optical Lattices, Phys. Rev. Lett. **91**, 080403 (2003).
[15] R. Roth and K. Burnett, Phase diagram of bosonic atoms in two-color superlattices, Phys. Rev. A **68**, 023604 (2003).
[16] G. Roati, F. Riboli, G. Modugno, and M. Inguscio, Fermi-Bose Quantum Degenerate ^{40}K – ^{87}Rb Mixture with Attractive Interaction, Phys. Rev. Lett. **89**, 150403 (2002).
[17] S. Lellouch and L. Sanchez-Palencia, Localization transition in weakly-interacting Bose superfluids in one-dimensional quasiperdiodic lattices, Phys. Rev. A **90**, 061602(R) (2014).
[18] L. Sanchez-Palencia and L. Santos, Bose-Einstein condensates in optical quasicrystal lattices, Phys. Rev. A **72**, 053607 (2005).
[19] N. Macé, A. Jagannathan, and M. Duneau, Quantum simulation of a 2D quasicrystal with cold atoms, Crystals **6**, 124 (2016).
[20] K. Viebahn, M. Sbroscia, E. Carter, C. Yu, Jr., and U. Schneider, Matter-wave diffraction from a quasicrystalline optical lattice, arXiv:1807.00823.
[21] L. Fallani, J. E. Lye, V. Guarrera, C. Fort, and M. Inguscio, Ultracold Atoms in a Disordered Crystal of Light: Towards a Bose Glass, Phys. Rev. Lett. **98**, 130404 (2007).
[22] B. Gadway, D. Pertot, J. Reeves, M. Vogt, and D. Schneble, Glassy Behavior in a Binary Atomic Mixture, Phys. Rev. Lett. **107**, 145306 (2011).
[23] L. Tanzi, E. Lucioni, S. Chaudhuri, L. Gori, A. Kumar, C. D'Errico, M. Inguscio, and G. Modugno, Transport of a Bose Gas in 1D Disordered Lattices at the Fluid-Insulator Transition, Phys. Rev. Lett. **111**, 115301 (2013).
[24] C. D'Errico, E. Lucioni, L. Tanzi, L. Gori, G. Roux, I. P. McCulloch, T. Giamarchi, M. Inguscio, and G. Modugno, Observation of a Disordered Bosonic Insulator from Weak to Strong Interactions, Phys. Rev. Lett. **113**, 095301 (2014).
[25] S. Iyer, V. Oganesyan, G. Refael, and D. A. Huse, Many-body localization in a quasiperiodic system, Phys. Rev. B **87**, 134202 (2013).
[26] A. Lukin, M. Rispoli, R. Schittko, M. E. Tai, A. M. Kaufman, S. Choi, V. Khemani, J. Léonard, and M. Greiner, Probing entanglement in a many-body-localized system, arXiv:1805.09819.
[27] R. Matthew, L. Alexander, S. Robert, K. Sooshin, T. M. Eric, L. Julian, and G. Markus, Quantum critical behavior at the many-body-localization transition, arXiv:1812.06959.
[28] T. Kohlert, S. Scherg, X. Li, H. P. Lüschen, S. Das Sarma, I. Bloch, and M. Aidelsburger, Observation of many-body localization in a one-dimensional system with single-particle mobility edge, arXiv:1809.04055.
[29] E. Abrahams, P. W. Anderson, D. C. Licciardello, and T. V. Ramakrishnan, Scaling Theory of Localization: Absence of Quantum Diffusion in Two Dimensions, Phys. Rev. Lett. **42**, 673 (1979).
[30] S. Aubry and G. André, Analyticity breaking and Anderson localization in incommensurate lattices, Ann. Isr. Phys. Soc. **3**, 133 (1980).
[31] C. M. Soukoulis and E. N. Economou, Localization in One-Dimensional Lattices in the Presence of Incommensurate Potentials, Phys. Rev. Lett. **48**, 1043 (1982).

[32] S. Das Sarma, A. Kobayashi, and R. E. Prange, Proposed Experimental Realization of Anderson Localization in Random and Incommensurate Artificially Layered Systems, Phys. Rev. Lett. **56**, 1280 (1986).
[33] S. Das Sarma, S. He, and X. C. Xie, Localization, mobility edges, and metal-insulator transition in a class of one-dimensional slowly varying deterministic potentials, Phys. Rev. B **41**, 5544 (1990).
[34] J. Biddle, B. Wang, D. J. Priour, and S. Das Sarma, Localization in one-dimensional incommensurate lattices beyond the Aubry-André model, Phys. Rev. A **80**, 021603 (R) (2009).
[35] J. Biddle and S. Das Sarma, Predicted Mobility Edges in One-Dimensional Incommensurate Optical Lattices: An Exactly Solvable Model of Anderson Localization, Phys. Rev. Lett. **104**, 070601 (2010).
[36] J. Biddle, D. J. Priour, B. Wang, and S. Das Sarma, Localization in one-dimensional lattices with non-nearest-neighbor hopping: Generalized Anderson and Aubry-André models, Phys. Rev. B **83**, 075105 (2011).
[37] S. Ganeshan, J. H. Pixley, and S. Das Sarma, Nearest Neighbor Tight Binding Models with an Exact Mobility Edge in One Dimension, Phys. Rev. Lett. **114**, 146601 (2015).
[38] A. Szabó and U. Schneider, Non-power-law universality in one-dimensional quasicrystals, Phys. Rev. B **98**, 134201 (2018).
[39] D. J. Boers, B. Goedeke, D. Hinrichs, and M. Holthaus, Mobility edges in bichromatic optical lattices, Phys. Rev. A **75**, 063404 (2007).
[40] X. Li, X. Li, and S. Das Sarma, Mobility edges in one-dimensional bichromatic incommensurate potentials, Phys. Rev. B **96**, 085119 (2017).
[41] L. Gori, T. Barthel, A. Kumar, E. Lucioni, L. Tanzi, M. Inguscio, G. Modugno, T. Giamarchi, C. D'Errico, and G. Roux, Finite-temperature effects on interacting bosonic one-dimensional systems in disordered lattices, Phys. Rev. A **93**, 033650 (2016).
[42] H. P. Lüschen, S. Scherg, T. Kohlert, M. Schreiber, P. Bordia, X. Li, S. Das Sarma, and I. Bloch, Single-Particle Mobility Edge in a One-Dimensional Quasiperiodic Optical Lattice, Phys. Rev. Lett. **120**, 160404 (2018).
[43] F. Evers and A. D. Mirlin, Anderson transitions, Rev. Mod. Phys. **80**, 1355 (2008).
[44] See Supplemental Material at http://link.aps.org/supplemental/10.1103/PhysRevLett.123.070405. It discusses the scaling analyses of the IPR and IDOS, the determination of the critical point V_c, the critical and fractal behaviors for the imbalanced bichromatic lattice, and the tight-binding and AA limits.
[45] The quantity $n_\epsilon(E)/\epsilon$ may be interpreted as the density of states (DOS) for an energy resolution ϵ. Because of the fractality of the energy spectrum, the DOS $\lim_{\epsilon\to 0_+} n_\epsilon(E)/\epsilon$ is, however, ill defined (see below).
[46] M. Kohmoto, Metal-Insulator Transition and Scaling for Incommensurate Systems, Phys. Rev. Lett. **51**, 1198 (1983).
[47] C. Tang and M. Kohmoto, Global scaling properties of the spectrum for a quasiperiodic Schrödinger equation, Phys. Rev. B **34**, 2041 (1986).
[48] M. Kohmoto, B. Sutherland, and C. Tang, Critical wave functions and a Cantor-set spectrum of a one-dimensional quasicrystal model, Phys. Rev. B **35**, 1020 (1987).
[49] T. Roscilde, Bosons in one-dimensional incommensurate superlattices, Phys. Rev. A **77**, 063605 (2008).
[50] B. B. Mandelbrot, *The Fractal Geometry of Nature* (W. H. Freeman, New York, 1982), Vol. 2.
[51] J. Theiler, Estimating fractal dimension, J. Opt. Soc. Am. A **7**, 1055 (1990).
[52] For a continuous (respectively, discrete) spectrum, one finds $D_H = 1$ (respectively, 0). Intermediate values of D_H are characteristic of a nontrivial self-similar behavior.
[53] P. Lugan, D. Clément, P. Bouyer, A. Aspect, M. Lewenstein, and L. Sanchez-Palencia, Ultracold Bose Gases in 1D Disorder: From Lifshits Glass to Bose-Einstein Condensate, Phys. Rev. Lett. **98**, 170403 (2007).
[54] I. M. Lifshits, S. Gredeskul, and L. Pastur, *Introduction to the Theory of Disordered Systems* (Wiley, New York, 1988).
[55] C. W. J. Beenakker, Random-matrix theory of quantum transport, Rev. Mod. Phys. **69**, 731 (1997).
[56] L. Pezzé and L. Sanchez-Palencia, Localized and Extended States in a Disordered Trap, Phys. Rev. Lett. **106**, 040601 (2011).
[57] V. V. Volchkov, M. Pasek, V. Denechaud, M. Mukhtar, A. Aspect, D. Delande, and V. Josse, Measurement of Spectral Functions of Ultracold Atoms in Disordered Potentials, Phys. Rev. Lett. **120**, 060404 (2018).
[58] J. Richard, L.-K. Lim, V. Denechaud, V. V. Volchkov, B. Lecoutre, M. Mukhtar, F. Jendrzejewski, A. Aspect, A. Signoles, L. Sanchez-Palencia *et al.*, Elastic Scattering Time of Matter Waves in Disordered Potentials, Phys. Rev. Lett. **122**, 100403 (2019).
[59] G. Roux, T. Barthel, I. P. McCulloch, C. Kollath, U. Schollwöck, and T. Giamarchi, Quasiperiodic Bose-Hubbard model and localization in one-dimensional cold atomic gases, Phys. Rev. A **78**, 023628 (2008).